PHYSICAL REVIEW B VOLUME 17, NUMBER 4 15 FEBRUARY 1978

Dangling bonds on silicon

B. P. Lemke and D. Haneman
School of Physics, University of New South Wales, Sydney, Australia 2033
(Received 28 May 1976)

The electron-paramagnetic-resonance signal that appears when Si is crushed, cleaved, or abraded is shown to be proportional to the areas of microcracks induced in the specimen. These are shown to be more prevalent than previously realized. Detailed consideration shows that a wide variety of previously inexplicable data can now be understood. These include some effects of oxygen and hydrogen, variability of signal width, effects of abrasive particle size, and kind of cleavage. The origin of the unpaired electrons is considered and it is concluded that they may be in localized states on the surfaces of the microcracks, such states being apparently a case of Anderson localization. The atoms on the crack surfaces are subject to spatially varying overlap forces and stress fields whose energy range exceeds the normal bandwidth, thus inducing localization. The temperature dependence of the paramagnetism of such states is discussed, including correlation corrections, and shown to yield approximately T^{-1}, as observed experimentally. A similar explanation applies to Ge. Clean-cleaved Si surfaces display negligible surface paramagnetism due to pairing of surface electrons on alternate atom sites. The results suggest that for amorphous Si and Ge, localized states on the surfaces of small atom aggregates should be considered as a possible source of the observed paramagnetism.

I. INTRODUCTION

A simple model of a (111) surface of a diamond-structure covalent semiconductor, such as in Fig. 1, shows one cut bond per surface atom, leading to the expectation of one electron in each such "dangling" bond. Such electrons, if remaining largely unpaired, should be detectable by electron paramagnetic resonance (EPR) measurements. Indeed, EPR signals have been found from Si, Ge, C, and Ge-Si surface regions.[1] It has been a point of major interest to determine whether the simple concept of Fig. 1 is largely correct, or whether the atomic rearrangements known to occur on most semiconductor surfaces cause major modifications. The dangling-bond concept has remained the simplest starting off point for many theoretical discussions of surfaces, and could not be seriously tested while surface structures remained uncertain. Recently, theoretical computations of surface states have been carried out self-consistently by Schluter and co-workers[2] for a surface model (Haneman)[3] leading to a conclusion of paired electrons on alternate sites. This would give only a very weak EPR signal. Recent EPR measurements[4,5] have shown that there is indeed a negligible EPR signal from well-cleaved Si surfaces. In this paper we report new evidence concerning the origin of the EPR signal that is observed on less well-cleaved surfaces, which we show to be due to localized states on microcrack surfaces. Hence the simple picture of Fig. 1 is not a correct description of cleaved covalent silicon and the simple concept of filled dangling-bond states must be treated with great caution.

II. EPR OBSERVATIONS

The original dangling-bond hypothesis had to be considered carefully for Si surfaces in particular since much data showed an EPR signal to be present in the surface region of this material. Most of the results to 1974 have been reviewed[1] and will not be described in detail here. In summary, an EPR signal at $g = 2.0055$, width about 0.65 mT, has been found at room temperature from Si surfaces that have been abraded, produced by crushing, by cleavage, irradiated with neutrons or high-energy ions, heated in vacuum and rapidly cooled, and from amorphous films.

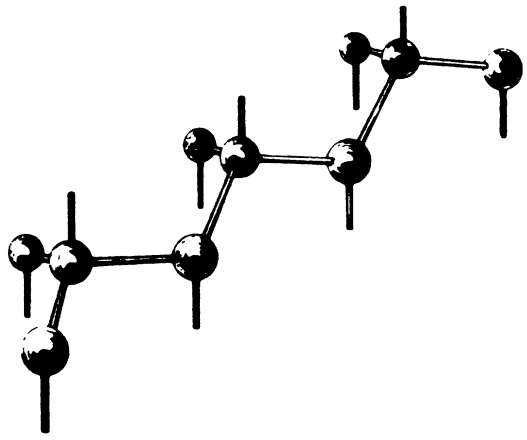

FIG. 1. Oblique view of ideal undistorted (111) surface of diamond structure material showing one broken bond per surface atom.

A variety of hypotheses were advanced regarding the origin of the signal, but all had serious shortcomings. Vacancy clusters or vacancy-impurity complexes within 10^{-4} cm of the surface were unable to satisfactorily explain why oxygen and hydrogen exposures (10^{-4} Torr min) affected the resonance. The Si *A* center (an oxygen atom captured by a vacancy) cannot exist in sufficient concentration in low-oxygen-content crystals crushed in ultrahigh vacuum to give the very high spin concentrations that are obtainable. Step edges have been suggested as EPR sites but these are known to be the most active sites for adsorption whereas the EPR signal is affected at exposures, orders of magnitude higher than those which affect ordinary surface properties (work function, photoemission).

We had earlier suggested that the surface itself contained two kinds of sites [associated with the 2 × 1 low-energy-electron diffraction (LEED) cell] — only one giving an EPR signal and having a lower affinity for gases than the other site. However, we have recently shown[5] that a well-cleaved surface has less than 1 spin per 1000 surface atoms. (Kaplan *et al.*[4] have also shown recently a density less than 1 spin per 100 atoms). The fact that the spin density from high-quality cleaved surfaces can be very much lower than for poorer surfaces points to an origin associated somehow with cleavage quality rather than with the flat surface. However, the existence of a sensitivity to gases suggests centers to which gas can arrive, yet not centers that are active, such as steps.

Analysis of these data led us to suspect that centers in microcracks might be responsible. In the remainder of this paper we shall describe: (i) circumstantial evidence for this, (ii) a series of test experiments, (iii) evidence for the widespread occurrence of microcracks, (iv) a more detailed hypothesis for the centers, and (v) extension to the case of amorphous films.

III. MICROCRACK HYPOTHESIS

One of the difficulties about the behavior of the EPR signal, and yet, a principal clue to its origin, is the behavior upon exposure to gas. As detailed previously,[3,6,7] oxygen and hydrogen begin to affect the signal noticeably (changes of a few percent) at exposures of 10^{-4} Torr min. This is in striking contrast to the behavior[8,9] of surface conductivity, photoemission, and work function, which are noticeably affected by oxygen at exposures of about 10^{-8} Torr min, and yet are only slightly, if at all, affected by molecular hydrogen. Surprisingly, the latter causes quite big changes to the EPR signal.

We have referred to changes in the EPR signal height, but its shape also changes. Hence an important question is what happens to the number of spin centers. This cannot be accurately deduced for the following reasons. In order to obtain the number of spins from an EPR signal one needs a theoretical expression relating spin density to signal strength. Such expressions[10] can be derived with confidence for two extreme cases: one when the spin centers are largely localized, giving a T^{-1} temperature dependence of signal strength, and secondly when the centers are in a reasonably wide conduction band, leading to T^{0} dependence. The Si signal from the clean surfaces varies close to T^{-1}, hence the number of spins is determinable. However, after gas exposure, the temperature dependence is T^{-n} where $0<n<1$, being different for oxygen and hydrogen.[6] Unless one has a theoretical expression for the observed temperature behavior one cannot deduce the spin concentration. Expressions for cases more general than localized or band states have been obtained,[11] but it is not clear that the assumptions involved are necessarily applicable to the present cases. Therefore we cannot reliably determine the number of spins after gas adsorption. However, since the signal strength is not very different, it is probable that the number of spins has not changed very much.

The fact that oxygen only affects the EPR signal at relatively high exposures, coupled with the fact that positive effects occur with molecular hydrogen, is strongly reminiscent of the behavior of surface barriers at closed splits. In those cases the gas effects were quite similar.[12] In Figs. 2 and 3 we plot changes in photovoltage across mated splits, together with inverse of EPR signal height, versus exposure to oxygen and hydrogen, respectively. The photovoltage is related to the heights of the surface barriers at the two surfaces of the small controlled partial splits, as shown in Fig. 4. The surface barrier heights are intrinsically just as sensitive to oxygen as properties such as photoemission. The reason for the apparently insensitive response of surface at cracks is that the effective pressure in a fissure is very much less than that on freely exposed surfaces. All molecules incident upon the mouth of the fissure are distributed over the areas of the sides of the fissure. It has been found[13] that carefully made and closed partial splits may have remanent jaw openings as small as about 1.5 nm, for split lengths of about 0.5 mm. This gives a ratio of fissure mouth to wall area of order 10^{-6} ($15\times10^{-10}/2\times0.5\times10^{-3}$). Hence an exposure of 10^{-4} Torr min only corresponds to an effective exposure of order 10^{-10} Torr min averaged over the fissure walls. The reasons that the cracks do not close completely are

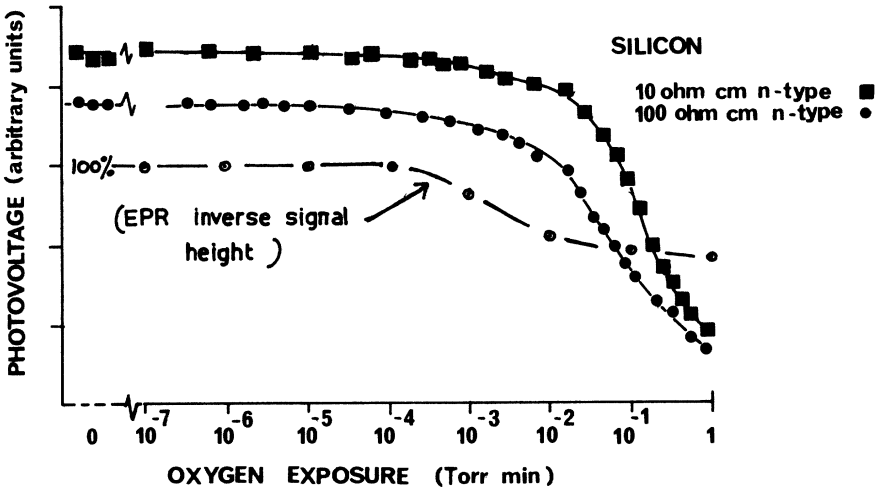

FIG. 2. Effect of exposure to oxygen upon maximum photovoltage developed when Si vacuum split structure of Fig. 4 is scanned with fine light beam (Ref. 12). Also shown is effect (Ref. 3) upon inverse of EPR signal height obtained from vacuum crushed Si. (1 Torr min $= 8 \times 10^3$ Pa sec.)

thought to be slight mismatch of surface irregularities near the crack mouth, due to shear of about 15–60 Å at the mouth, measured by transmission x-ray topography.[13] In general, cracks would not be as perfect as those specially made in the above referenced studies, and could be held open to greater extents due to greater shear. Hence the ratio of fissure mouth to side area would be in general greater than 10^{-6}. These factors readily explain the apparently slow gas exposure effects on the photovoltage . They also explain the sensitivity to molecular hydrogen since such molecules entering the fissures would be channeled down, and consequently held in close proximity to the crack surfaces for much longer than on free surfaces where the molecules can at once bounce right off. This is indicated schematically in Fig. 5.

The general correspondence of the above gas effects with those on the Si EPR signal shown in Figs. 2 and 3 leads one to suspect that the EPR

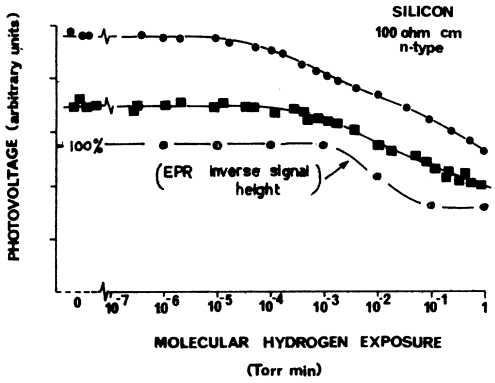

FIG. 3. Same as for Fig. 2, but exposure to hydrogen.

centers might also be located at cracks. To test the hypothesis one would ideally induce cracks of various sizes and measure any corresponding EPR signals. This could not be done for a single controlled crack since the EPR signal was too small to study properly. Hence it was necessary to prepare multiple cracks.

IV. EPR MEASUREMENTS ON INDENTED SPECIMENS

It is known that indentation of Si and other brittle materials with a hard conical or diamond shaped point produces cracks. The nature of the damage is shown in Fig. 6. Two roughly semicircular penny shaped cracks (nearly orthogonal to each other and the surface) are produced as the point presses down, and a few cusp shaped cracks are produced as the point is released. The former are known

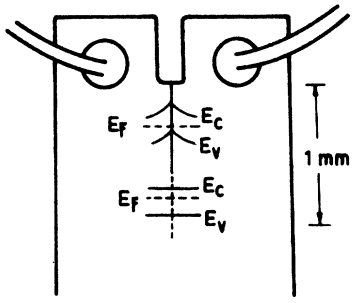

FIG. 4. Diagram of n-type semiconductor specimen with partial split initiated from groove at top. Energy bands at top region show barriers at surface-to-surface contact, giving effective npn region; at bottom the crystal has healed. Metallic ohmic contacts are shown at top of specimen. These deliver a voltage when light impinges on specimen on either side of, and adjacent to, the split. From Grant and Haneman (Ref. 12).

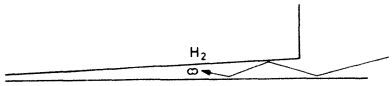

FIG. 5. Schematic diagram showing entry and temporary entrapment of hydrogen molecules in split.

as median vents and the latter as lateral vents.[14] In addition there is a region of crushed material just under the point.

For a proper study it was necessary to remove the crushed material so that any EPR signal could be more definitely associated with the large cracks. (The crushed material is full of small cracks.) This was achieved by ultrasonic cleaning in distilled water. This process removed all debris visible under a scanning electron microscope, from the surface, and also from the central indentation pit. It also completed many of the lateral vent cracks so that the relevant pieces were removed. The effect is shown in the scanning micrographs in Fig. 7.

Experiments were performed by taking Si surfaces cleaved in air, giving them a light etch, and then making a series of indentations with a Zwick Hardness Tester (Z.3.2 A) using a diamond pyramid indenter. To obtain a sufficient EPR signal it was necessary to make at least 50, and in the case of light loads up to 250, indentations on each surface. This also averaged out the unavoidable slight differences between the indentations. Their spacing was about twice the visible crack extent, to reduce the effects of neighboring stress fields modifying subsequent cracks. The specimen was cushioned on a soft tissue during pressure. The corners of the diamond pyramid indenter pointed in the ⟨110⟩ and ⟨112⟩ directions, and the same orientation was always used.

The EPR signal was measured in air before and after ultrasonic cleaning. The signal height after the latter process (which reduced the signal as expected due to removal of crushed fragments)

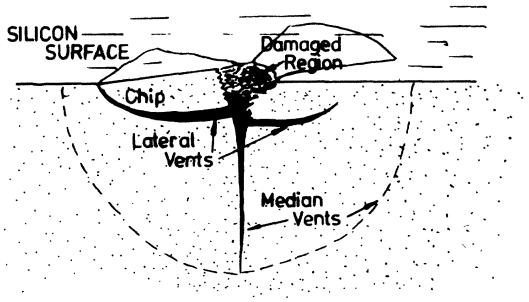

FIG. 6. Schematic diagram, sectional view, of damage region after point indentation.

(a)

(b)

FIG. 7. Scanning-electron-microscope pictures of diamond point indentation (1 kg load) on (111) Si surface (a) before and (b) after ultrasonic cleaning. Note removal of powder debris and lifting out of portions on lateral vent cracks. Width of micrograph, 0.17 mm.

was plotted as a function of indenter load P. This did not give a straight line. Several trial plots were made and it was found that a straight line ensued if EPR signal S was plotted vs $P^{4/3}$, as shown in Fig. 8. Now independent studies of crack size D (the radius of the penny shaped median vents) in brittle materials have been carried out as a function of indenter load P. The results of Lawn and Fuller[15] shown in Fig. 9 indicate $P \propto D^{3/2}$. This result is also expected theoretically. Since

$$S \propto P^{4/3},$$

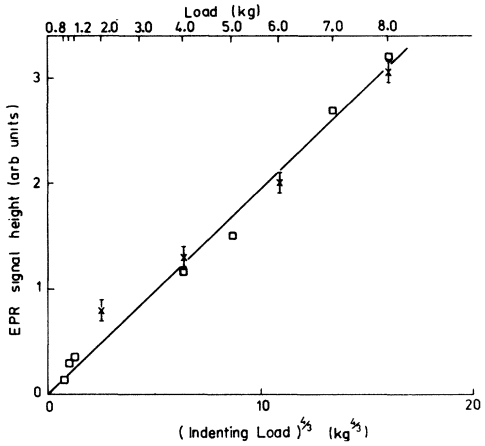

FIG. 8. Graph of EPR signal height, averaged per indentation, versus $\frac{4}{3}$ power of load on diamond point indenter.

one has

$$S \propto (D^{3/2})^{4/3} \propto D^2 \propto A ,$$

where A is the area of the crack. Hence these studies, carried out for a very large number of indentations and an extensive range of pressures, show that the EPR signal is proportional to the area of the median vent cracks. (The lateral vent cracks which still remain after ultrasonic cleaning contain much less crack area than the median vents and can be neglected. Their area is in any case probably related linearly or nearly so to that of the median vents so that the above relationship would be unaffected.)

Having established this connection between EPR signal and crack area, we now test the hypothesis against another class of results that have never hitherto been satisfactorily explained.

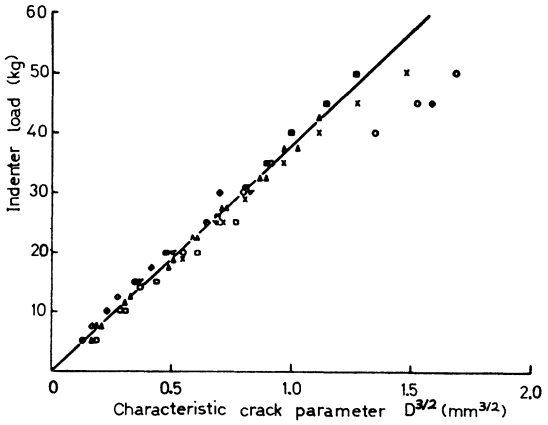

FIG. 9. Graph of indenter load versus $D^{3/2}$ where D is radius of median vent shown in Fig. 6. From Lawn and Fuller (Ref. 15).

V. EPR FROM ABRADED SPECIMENS

When Si samples are abraded, the above characteristic EPR signal results.[16-18] Experiments were repeated here on surfaces of various orientation. Ten Si strips ($20 \times 3 \times 0.5$ mm^3) were cut at 10° intervals from the (111) face to the (110) face and were than abraded on both opposite (large) faces with 6-μ diamond grit. To within experimental error the EPR signal from all the strips was the same. This independence of gross face orientation is expected if the major EPR effect of abrasion is to induce cracks, since these will be mostly along (111) planes regardless of the face abraded.

When abrasive particles of different size are used, the EPR signal is altered. Measurements of these effects were first performed by Taloni and Rogers,[19] Fig. 10. We obtained similar results using, as they did, diamond grit. Both curves in Fig. 10 show a peak EPR signal after abrasion with particles of about 7-μ size. (Note that carborundum particles have a greater size variation from the nominal than do diamond particles, and give less sharp results).

Also shown in Fig. 10 is the average damage depth, measured by SEM (scanning electron microscope) metallographic techniques, and the surface area, measured with a Talysurf probe technique. Both the average damage depth and surface area increase monotonically with abrasive particle size, as expected, but this is in sharp contrast with the behavior of the EPR signal. The latter reaches a peak followed by a slight decrease and then a leveling off which could not be understood. However, in terms of the microcrack hypothesis the behavior is explicable if the micro-

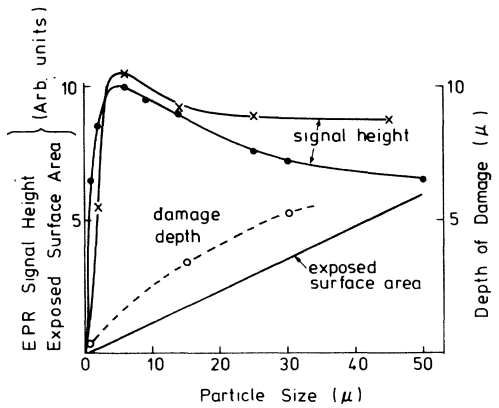

FIG. 10. Effect of grinding with different particle sizes (abscissa) on three different parameters, EPR signal height, exposed surface area, and depth of damage (average). Uppermost curve, this study; others from Taloni and Rogers (Ref. 19).

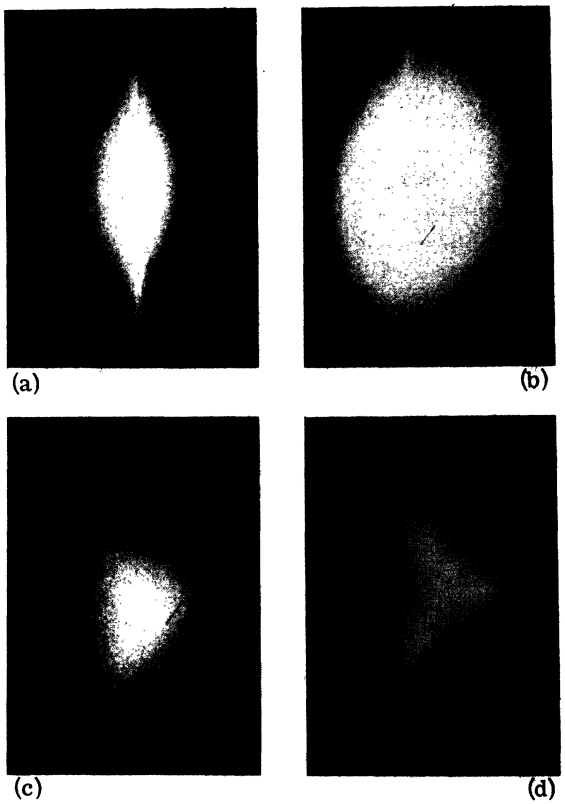

FIG. 11. Appearance on screen of laser beam reflected at normal incidence from mechanically polished Si specimens. Polishing particle sizes in microns, (a) 1, (b) 6, (c) 14, (d) 25.

crack area does not increase after approximately 7-μ abrasive particles are used. The explanation is, as we shall show, that as the cracks increase in size they join together, at which point whole pieces (chips) are removed from the surface. Thus these cracks disappear. Heavier abrasion continues this process of (111) cracks joining to give pyramidal pits, with no net increase in crack area, even though the average damage depth continues to increase.

The above hypothesis was tested by examining the reflection of a laser beam incident normally on each surface. The patterns are shown in Fig. 11. Note that for very small particle abrasion only a diffuse reflection occurs. However, after about 14-μ particles a triangular reflection pattern is discernible and becomes more distinct with rougher abrasion. This clearly shows that three-sided pyramid pits are forming, due to confluence of (111) cracks on the (111) surface. This thus supports the above explanations.

Some further evidence consistent with this explanation was obtained by heating the Si samples in air. Two samples were used, one abraded with 6-μ and the other with 25-μ particles. The effects of heating are shown in Fig. 12. Note that the 6-μ sample signal is initially larger than that of the 12-μ sample, but after annealing at progressively longer times, it eventually reduces to about the same value. (The initial rise for both samples in Fig. 12 may be due to further cracking.) Now the 12-μ sample is known to contain deeper cracks than the 6-μ sample due to the rougher abrasion. These cracks, however, are fewer in number since more crack confluence to make chips has occurred, hence the EPR signal is initially smaller than for the 6-μ sample, as shown also in Fig. 10. Since the samples are heated in air, heavy oxidation of the surfaces on the cracks will occur, destroying the signal. Such oxidation would be expected to affect shallower cracks before the deeper parts of the deeper cracks can be attacked. Hence one expects the 12-μ sample signal to survive the air oxidation better than the 6-μ signal. This is consistent with the behavior in Fig. 12 where the final signal for the 12-μ sample is about 26% of the original whereas the final 6-μ signal is only about 20% of the initial value.

VI. EVIDENCE FOR EXISTENCE OF MICROCRACKS

Direct evidence for existence of microcracks on abraded surfaces has been obtained in the past by taper section techniques. When a taper section is chemically etched, cracks intersecting the section surface are displayed. A typical result[20] is shown in Fig. 13.

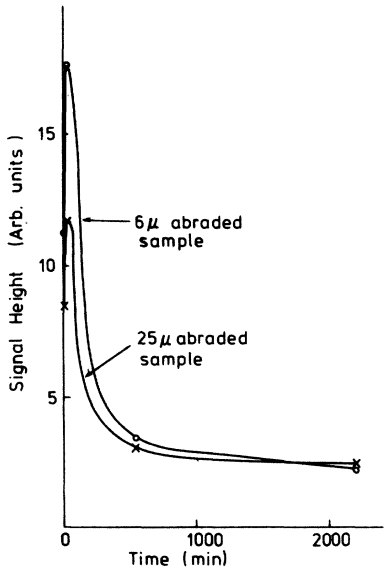

FIG. 12. EPR signal height measured at room temperature versus time of anneal at 300 °C, for samples abraded with particles of size 6 and 25 μm.

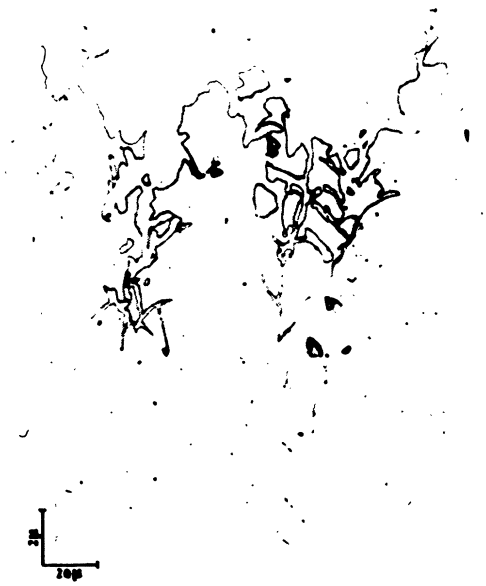

FIG. 13. Taper section (10:1) of surface abraded with 220 grade SiC and etched with CP4(HF:CH_3COOH:HNO_3:Br in the ratios 50:50:80:1), showing microcracks. From Pugh and Samuels (Ref. 20).

In the case of crushed powders, the particles are produced by extensive mechanical abuse and contain very rough and jagged surfaces. When these are examined by scanning electron microscopy, numerous cracks are clearly visible. The nature of many of these can be found by studying rough

FIG. 14. Scanning electron micrograph of surfaces of crushed powder particle, showing cracks between regions of different morphology. Width of picture, 240 μm.

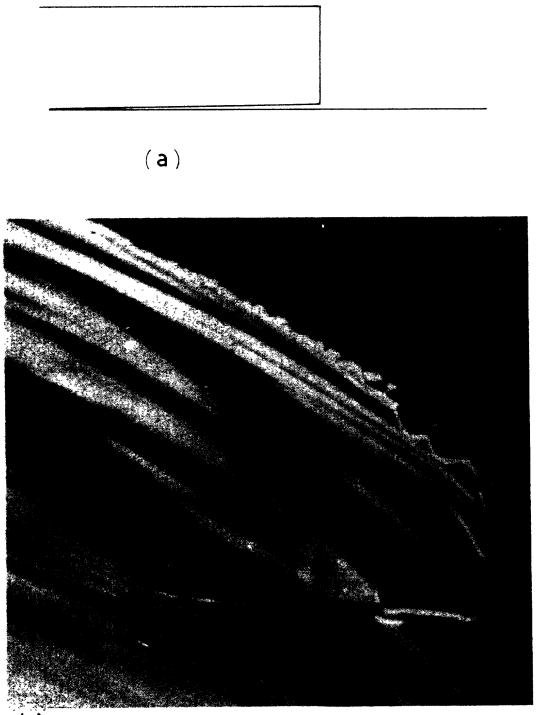

FIG. 15. (a) Schematic drawing of crack under step. (b) Scanning electron micrograph of steps on cleaved Si surfaces, revealing undercracks where piece chipped off. Width of picture, 200 μm.

cleavage areas, as shown in Fig. 14. Note the fissures that separate regions of different topographical patterns. In the case of better cleaved areas, cracks are still present. In such cases they were found to occur under macroscopic (order micron step height) steps. Thus in quite a few cases steps were found to consist of overhangs as shown in Fig. 15. This was determined in two ways. First some of the fissures under the steps were directly visible by SEM as shown. The fissure presence could be confirmed by extensive tilting of the specimens on the SEM stage (Cambridge Mark II). Secondly the step overhang structure could be revealed by direct probing with a very fine tungsten point under an optical microscope. When the point was pressed hard against a step, in several cases (order 10–20%) quite a slight pressure caused the step to flake off.

The reasons for the presence of undercuts on steps have to do with the mechanism of crack progression during cleavage. It has been argued that cleavage initiates at several points on different planes. As the cracks spread across these planes, at certain points the material breaks between them, leading to a step edge with an extensive undercut. Evidence for this is discussed in

FIG. 16. Scanning electron micrograph of top portion of Si crystal showing chipped region induced by wedge forced into groove. Specimen did not break at groove, but gave EPR signal after this damage. Specimen approximately 5×2 mm^2 cross sectional area.

the fracture literature.[21]

It is not easy to determine the degree of undercutting in steps by visual inspection in an optical microscope. It is necessary to perform SEM inspections. To find the narrower fissures under steps, mechanical probing is useful.

The ease with which misleading EPR results can be obtained is illustrated by the appearance of the sample in Fig. 16. This sample was one of those used in the single-crystal ultra-high-vacuum cleavage experiments described earlier.[5] A conical wedge inserted in the prepared groove was struck with a weight, but cleavage did not take place. Nevertheless, some chipping and cracking occurred, as shown. This gave a relatively strong EPR signal. It is believed that such areas were present on specimens used in earlier experiments,[3] where the EPR signal was averaged over the visible cleavage surface area, yielding a certain number of spins per free surface area. In fact the free surface area was largely irrelevant since we now know that the signal came mostly from regions of large crack density.

We now estimate the spin density in the microcracks. From the results of the indentation experiments described in Sec. IV one could measure the total number of spins and the total area of surfaces in the median vent cracks. Errors in spin numbers have been discussed previously[10] and are at least 50%. The median vent areas were estimated by assuming the visible crack mouths were diameters of semicircular cracks beneath the surface. From the sectional appearance of such cracks, this assumption is reasonable. The lengths of the mouths varied by about 50% over the various ostensibly identical indentations, hence an average length was taken. Taking into account two surfaces per crack, the number of spins per surface area of crack was 10^{14} spins cm^{-2} for indentations of 2–8 kg load. The error is estimated as about a factor of 4, due to errors in spin counts and in the area estimates.

We now enquire as to the basic nature of the spin centers.

VII. ORIGIN OF SPIN CENTERS IN MICROCRACKS

The experimental results show: (i) the $g=2.0055$ spin centers are located in microcracks, and are gas accessible; (ii) the number of spins is proportional to the area of crack; (iii) the number of spins per unit area of crack is about 10^{14} cm^{-2} to about a factor of 4; (iv) the spin density from cleaved surfaces[5] is less than 10^{12} cm^{-2}.

These facts set limits to possible models for the EPR centers. Consider first the possibility that they are located on microscopic debris of size order angstroms, since they are not visible by SEM. (SEM-visible debris is removed by ultrasonic cleaning.) Now if such debris is formed in cracks, when the cracks are opened to reveal the surfaces, the EPR signal should still be present since visible debris is observed to cling to surfaces. However, many experimental trials[4,5] show that well-cleaved surfaces (which must initially be in a crack) usually give negligible EPR signal, less than 10^{12} cm^{-2}, whereas cracks give signals of order 10^{14} spins per cm^2 of crack surface. Hence to account for the results one must postulate microscopic debris in cracks on abraded and indented specimens which is present in 100 times greater concentration than on surfaces produced by carrying cracks through completely. This seems unreasonable, and one concludes that the EPR signal is not due to such debris. (Large debris of course gives an EPR signal because it is loaded with cracks.)

A second possibility concerns single and multiatom vacancies, interstitials, and impurities. Now ordinary bulk defects can be ruled out since the EPR signal in question arises *after* cracks are formed. Hence any defect complexes must be ones induced by the cracking. Further, molecular hydrogen has negligible effect on surface potential barriers[8,9] so any centers beneath surfaces would not be affected by hydrogen. It could, however, affect centers on the crack. Hence since hydrogen affects the EPR signal, Fig. 3, the centers are on

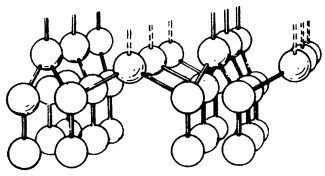

FIG. 17. Model[Haneman (Ref. 3)] of cleaved (111) surface of Si, showing alternate raised and lowered rows and strain-relieving shifts in second layer. Atom shifts are shown schematically (greatly exaggerated). Values (Ref. 22) used for Fig. 18 were raised, 0.018 nm; lowered 0.011 nm. Filled and empty bonds shown by full and dashed lines, respectively.

the crack surfaces. We thus must consider vacancy (or interstitial) groups intersecting the crack surfaces. This in effect corresponds to order atom sized pits, with presumably corresponding debris. But since one needs about 10^{14} spins cm^{-2} of fissure surfaces, one needs a corresponding density of defect complexes, which means the fissure surfaces consist mostly of defects. Yet cleavage surfaces that are free show excellent low-energy-electron diffraction patterns[9,23] indicative of negligible disorder. Such cleavage surfaces are themselves initially on fissures. They thus should not differ in defect quality from surfaces at partial splits that have not been carried to completion. We thus consider that defects on fissure surfaces are not present to any marked degree.

This leaves a third possiblity, that the EPR centers are on the normal fissure surfaces themselves. Since free cleavage surfaces show no EPR signal, one deduces that the electron state distribution on a cleavage surface may be disturbed while an opposite cleavage surface is in very close proximity to it. This disturbance might cause some kind of state localization leading to EPR centers. It is therefore necessary to consider this possibliity in detail.

A starting point is a knowledge of a free cleavage surface of Si, which may have the structure[3] shown in Fig. 17 (H model). This structure is consistent with a variety of experimental evidence.[23–25] It features alternate rows of atoms which are raised and lowered, leading to a 2×1 unit cell as observed by LEED. Recently several calculations[2,26–32] have been made concerning this model which we discuss briefly in the appendix. The band structure has been calculated self-consistently and is shown in Fig. 18.

In the case of clean-cleaved Si of high purity, the Fermi level is about 0.3 eV above the valence-band edge,[9] i.e., near the bottom of the upper surface band. Hence the consequence of the results in Fig. 18 is that the raised atom surface states, being well below the Fermi level, are fully occupied whereas the lowered atom surface states are largely empty. This double occupancy of the raised atom sites might possibly be more difficult than Fig. 18 indicates, due to charge repulsion, i.e., the surface bands might be split. On a Hubbard-type treatment[11] the splitting is approximately equal to the self-interaction energy of two electrons on the one site, screened by other electrons. If this occurred to any appreciable extent however, one would have a considerably stronger EPR signal, which should be detectable, and this is not observed from the crack-free surface. Hence splitting may not occur.

The surface states in Fig. 18 would give a negligible EPR signal since the lower band is practically full and the upper band largely empty. There would be small contributions from the latter due to the Fermi tail occupancy, but numerical estimates[11] place any such EPR signal as below current detection ability, even for large area powdered Si. Hence the absence of an observable EPR signal is fully consistent with the model and calculations.

The situation is altered when two such surfaces are placed opposite each other in close proximity as in a crack. Then the wave functions of the surface electrons on one side can overlap with those on the other side. The charge density contours of outer electrons on surface atoms have been computed.[2,33] They become very small (few percent of maximum value) at a distance of about 0.25 nm from the nucleus, so that overlap at a spacing of more than 0.5 nm becomes very small. A similar conclusion is reached from calculations of wave-function overlap at two spacings performed previously.[34] As shown in Fig. 19 the overlap is most for the case of in-line p orbitals, but even in this case it becomes slight after about 0.5 nm. Hence in order for appreciable effects to occur, the spacing between the surfaces must be less than about 0.5 nm. (These remarks refer to $\langle\psi|\psi\rangle$ whereas the important quantity is $\langle\psi|H|\psi\rangle$ where H is the interaction Hamiltonian. The latter is harder to calculate but its range will be similar to that

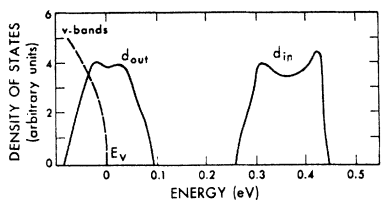

FIG. 18. Density of states for model (Ref. 3) and parameters (Ref. 22) of Fig. 17, calculated by self-consistent pseudopotential method for repeated 12 layer slabs. From Schüter, Chelikowsky, Louie, and Cohen (Ref. 2).

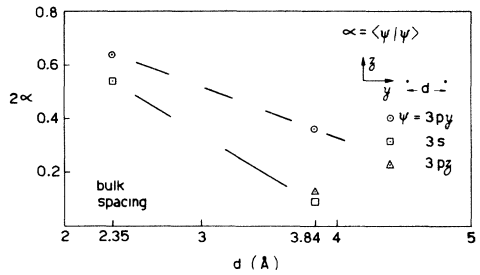

FIG. 19. Wave-function overlap $\langle\psi|\psi\rangle$ as function of spacing of nuclei, for various atomic wave functions. At bulk spacing of Si, 0.235 nm, $2\alpha = 1.34$ for sp^3 functions. From calculations of Haneman and Heron (Ref. 34).

of $\langle\psi|\psi\rangle$.)

This figure enables us to make a quantitative check. For special controlled cracks studied by x-ray transmission topography,[13] the jaws of an approximately 0.5 mm long crack could be as little as 1.5 nm apart, due presumably to slight step mismatch (there was a measurable shear of about 20 nm at the jaws). The shape of the crack sides for such cases is not readily calculable exactly, but will be similar to parabolic. Let half the spacing of the sides be y, at a distance x from the crack tip, as in Fig. 20. Then we may put $y = ax^2$ and, taking the above case $y = 0.8$ nm at $x = 0.5$ mm, one deduces $a = 3.2 \times 10^{-3}$ m^{-1}. At $y = 0.25$ nm, $x \simeq 0.28$ mm, i.e., 60% of the crack has a spacing of less than 0.5 nm. Hence in general about 50% of the crack is in a condition of wave-function overlap. If the microcracks are not much different from the controlled cracks, there is therefore ample scope for an EPR signal corresponding to 10^{14} spin cm^{-2}, as discussed in Sec. IV, provided there is something like one unpaired spin per several surface atoms in the overlap region. Most microcracks are much shorter than 0.5 mm, so that the overlap extent would be even greater. However, they are produced under rougher conditions than those used in the above experiments where the material was very carefully separated. Hence in naturally occurring microcracks, shear and other distortions are likely to be greater, so that the jaw openings might be relatively larger, than by extrapolating from the above figures. Even so, a sizeable proportion of a crack must have sides within about 0.5 nm, if it is only a small fraction of a mm long.

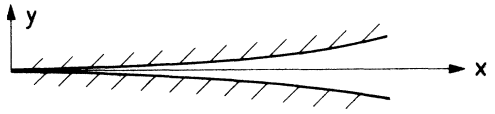

FIG. 20. Schematic diagram of crack.

A. Properties of overlap regions

We now consider the properties of the overlap regions in detail. At the very base of the split, as indicated schematically in Fig. 21(a), we have a transition from a healed region[35] to one with a finite gap. Now the two sides of the split are subject to three effects: (a) the separation increases towards the mouth; (b) the original registry between them on an atom-to-atom basis becomes lost due to shear, Fig. 21(b), since even the carefully prepared controlled splits showed measurable shear in the nonhealed region. In those cases values[13] ranged from 2.4 to 8×10^{-6} rad, giving about 3 nm displacement at the mouth of a 0.5 mm split, and thus more than 0.1 nm over most of it. Hence atoms are no longer opposite their precleavage neighbors; (c) contact regions exist at the edges of topographical irregularities[36] such as steps[37,38] on the faces of the split, and these are centers of pressure causing deformation of the material, Fig. 21(c). The result of these three effects is that, even in the 0.5 nm region of separation, the set of displacement vectors to opposite surface neighbors for any surface atom varies from site to site. Any individual atom is thus subject to forces from atoms on the opposite surface, but these forces vary from site to site since the shear displacement and separation vary (increase towards the jaw mouth), and the stress displacement varies also, being centered at somewhat random points and lines. This is a situation of varying potential which is of the kind considered by Anderson[39] and others. It is hence a possible practical example of Anderson localized sites.

B. Localized states

The criterion for Anderson localization has been discussed by various authors.[39–44] The consensus

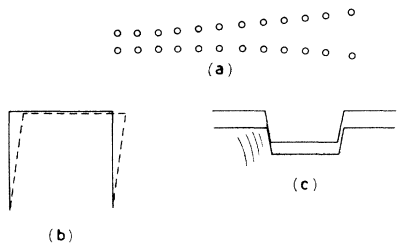

FIG. 21. (a) Schematic appearance of base of crack showing transition from healed to separated region. (b) Top view of crack, showing shear of one side with respect to other. (c) End view of crack showing pressure at contact between schematic protrusion on one side and corresponding gap on other.

is that localization occurs if the halfwidth of the distribution of potentials is greater than the width of the band resulting if all potential were the same. Consider the present case. The normal surface state band has a width[8,9] of about 0.3 eV. The potential disturbance due to the varying overlap can be estimated for comparison with this figure. At the base of the crack the overlap is strong, close to bulk, and will be in the region of the single bond energy in bulk Si, namely 2.37 eV.[45] When separation of the crack sides is more than 0.5–0.6 nm, the overlap approaches zero. Hence the range of potential disturbance is over 2 eV. This easily exceeds 0.3 eV. It thus fits the localization criterion. We must next determine whether such states give an EPR temperature dependence of T^{-n} ($n = 0.8$–1) as observed. (The uncertainty in n is due to caution concerning proper integration of nonstandard line shapes.)

C. Temperature dependence of spin paramagnetism from localized states

The temperature dependence of the paramagnetism from Bloch states in Hartree-Fock theory has been calculated. For the case of electrons on surface atoms it has been shown that correlation effects are important and a correction such as that of Hubbard is needed.[11] The T dependence of the EPR signal has been calculated for such cases.[11] In general a dependence close to T^{-1} is only obtained if a band surrounding the Fermi level is very narrow. In the case of localized states correlation effects are just as important. A solution for such a case has been obtained[46] using a few simplifying assumptions. The starting equation used by T. A. Kaplan and co-workers is[46]

$$H = \sum_i \sum_\sigma \epsilon_{i\sigma} N_{i\sigma} + \frac{1}{2} \sum_\sigma \sum_i U_i N_{i,+\sigma} N_{i,-\sigma} \quad (1)$$

where

$$\epsilon_{i\sigma} = \epsilon_i - f\sigma, \quad f = \tfrac{1}{2} g \mu_B B , \quad (2)$$

with B the magnetic induction, μ_B is the Bohr magneton, ϵ_i are the one-electron energies for N_s orthogonal localized states i, $N_{i\pm\sigma}$ are the fermion occupation number operators for states i and spin $\pm\sigma$ (spin up, +, or down, −), and U_i is the repulsive Coulomb energy between two electrons in the one localized state. The term with U_i is the form assumed by Hubbard and others. It was then assumed that U was constant, U_0, for all states, with

$$W(\epsilon, U) = W(\epsilon)\delta(U - U_0) , \quad (3)$$

where $N_s W(\epsilon) d\epsilon$ is the probability of finding the ϵ_i of Eq. (2) between ϵ and $\epsilon + d\epsilon$. In the case of low field, $f \ll kT$, and taking the case where $kT \ll U_0 < \Delta$ where Δ is the bandwidth centered at $\epsilon = 0$, they found the magnetic susceptibility

$$\chi = \frac{g^2 \mu_B^2}{4kT} N_s \int_{\mu - U_0}^{\mu} W(\epsilon) d\epsilon + \ln 2 [W(\mu) + W(\mu - U)] , \quad (4)$$

where μ is the Fermi level, [Eq. (4) is a numerically corrected version of that in Ref. 46]. The self-interaction energy U_0 is usually of the order of an eV so the condition $kT \ll U_0$ is satisfied up to room temperature and somewhat higher, and the term f is of order 10^{-4} eV at X-band EPR. This is much less than kT in the temperature range from liquid nitrogen to room, where our results for high vacuum crushed samples were obtained in clean condition. (Contamination alters the temperature dependence.) Hence $f \ll kT$. (The condition $U_0 < \Delta$ above is not essential since $U_0 > \Delta$ gives the atomic limit where χ is also proportional to T^{-1}.) Hence Eq. (4) is applicable. The magnitude of the second term in the equation is not far from ln2 as the factor $[W(\mu) + W(\mu - U)]$ will only be a small number. Thus this term is negligible compared to the first term, and this varies as T^{-1}.

In the specific case of a square density of states of width Δ, one obtains

$$\chi = \frac{g^2 \mu_B^2}{4} \frac{N_s}{\Delta} \left(\frac{U_0}{kT} + 2 \ln 2 \right) , \quad (5)$$

where clearly U_0/kT is much larger than $2 \ln 2$. It is thus found that the susceptibility varies as T^{-1}. This is in accord with the experimental results.

Although this theoretical result is satisfactory it must nevertheless be looked at critically. Equation (1) contains a correction for self-interaction energy for two electrons on the same site but not for the interaction U_{ij} on nearest neighbors. This was justified by inferring in effect that localized states were situated spatially among extended states and were thus sufficiently separated for U_{ij} to be small. (It has been argued that there are fewer localized states in the center region of a band than in the band tails.) In the crack surface case, localized states may be less separated by extended states and Eq. (1) should include a term

$$\sum_\sigma \sum_{\sigma'} \sum_{i,j} U_{ij} N_{i,+\sigma} N_{j,-\sigma'} ,$$

where i and j are the nearest neighbors. It is then necessary to estimate the effect of this term on the results.

A one-dimensional treatment for noninteracting Wannier sites[47] gave unpaired spins only if $U_0 > 2J$ where J was the value of U_{ij}, assumed constant.

A three-dimensional band case has been considered by Bari.[48] He took, as above, one electron per site, assumed all ϵ_i to be the same, took all U_i as the same, called U_0, and all U_{ij} as the same, called J. He also assumed a constant number of neighbors, z, for each site but considered equal numbers of two kinds of site α and β where α was surrounded by β and vice versa. The energy for one electron on each site was E_u and for paired electrons on alternate sites was E_p. He obtained

$$E_u = \tfrac{1}{2} z NJ, \quad E_p = \tfrac{1}{2} NU_0 . \tag{6}$$

Therefore to get an unpaired state one requires

$$E_u < E_p, \quad \text{i.e.,} \quad zJ < U_0 . \tag{7}$$

The above treatment has been extended by Miller in our laboratory to permit E_i to vary over the sites, giving a bandwidth Δ (constant density of states). Replacing operators on nearest-neighbors sites by expectation values, he finds[49] the criterion for unpaired states as

$$J < (U_0 + \Delta)/2z . \tag{8}$$

When J is included in Eq. (1) it is found that electrons pair to give zero paramagnetic susceptibility unless

$$2zJ - U_0 < \Delta , \tag{9}$$

which is the same as condition (8). With this restriction it may be shown,[49] by reasonable approximations to the Hamiltonian, that the expression for the susceptibility is identical with Eq. (5), i.e., it varies as T^{-1}. If the atom sites are on a (111) surface, the two kinds α and β can no longer surround each other. Now each α is surrounded on the surface plane, taken flat, by 4β and 2α, and vice versa. In this case it is easy to show that the effective value of z above is 2. Hence the condition for T^{-1} dependence is

$$J < \tfrac{1}{4}(U_0 + \Delta) . \tag{10}$$

While U_0 is not known precisely, this condition implies J less than about 1 eV, which is not unreasonable since J, being the interaction energy for electrons on neighboring sites, is considerably less than U_0.

D. Signal parameters and gas adsorption

We now consider further properties of the EPR signal in the light of the microcrack hypothesis. One of the previously puzzling features was that the signal width seemed to vary slightly from crushed sample to sample. The variation was about ±0.05 mT or slightly more, around a mean of about 0.65 mT. Now the number and type of crack (depth, shear) varies between samples. The EPR signal depends on the states of the localized electrons which in turn depend on microcrack properties such as separation between surfaces, their relative shear, the stress fields etc. Hence some minor variation in the EPR signal from different samples is not surprising.

Other data are also now explicable. Thus Shiota and co-workers[50] reported a 2.0055 signal in Si that has been heated and then cooled rapidly. It is known[51] that such treatment can cause cracks. Hence the occurrence of their signal is now easily understood. In the case of heavily irradiated Si,[52-54] the presence of the 2.0055 signal is usually explained as due to the rendering of the material into an amorphous condition by the extensive lattice disturbance. The reason for amorphous material giving the signal is explained in Sec. VIII.

With regard to the effects of exposure to oxygen, as detailed in Sec. III, the temperature behavior is altered and hence the number of spins becomes uncertain. However, the signal does become narrower by about 15% and also increases in height such that the area under the absorption curve remains about the same. However, the details of the interaction between oxygen and localized states (or other possible centers) are not known at this stage and hence a detailed discussion would be too speculative.

Similar remarks apply concerning interaction with hydrogen. It is interesting to note in this connection that hydrogen incorporated during the sputter formation of Ge films[55] did not affect the EPR g value. The line shape and width and temperature dependence of the width were, however, altered. These three features apply also to the effects on the EPR signal from crushed Si, when molecular hydrogen is introduced. The present authors therefore believe that it is possible that the above effects on Ge films may have been due, at least in part, to molecular hydrogen. (It was shown[55] that atomic hydrogen destroyed the EPR centers.)

VIII. AMORPHOUS FILMS

It has been known for some time that amorphous films[54-58] of Si and Ge give the same kind of EPR signal as crushed crystalline samples. The signal has been ascribed to centers in voids.[56] We believe the evidence and interpretations in this paper may have a bearing on the interpretation of amorphous film EPR results, due to the closeness of the correspondence of the signals from the two cases. Thus for Si, both films and crushed crystals have a g value of 2.0055, and a width close to 0.6 mT, although broader signals can be ob-

tained under some conditions. The signal shape is reported as Lorentzian for the films[56,57] but slightly broader (for a given peak height) than a Lorentzian shape for the crystals.

In view of this overall correspondence of the signals, one suspects similar centers. For the crystals the signal is here ascribed to localized states due to disorder on the surfaces of fissures. Since amorphous films are disordered throughout, it seems natural to consider localized states on the surfaces of the small aggregates of which the films are composed.[59] The centers are then gas accessible, in accordance with observations.[55,60]

Quantitative considerations are possible. The experimentally observed signal,[56] using a formula for isolated centers, corresponds to about 2×10^{20} centers cm^{-3} of material, independent of film thickness, which is one spin per 250 atoms. If the aggregates are regarded as spheres or cubes, the ratio γ of surface to bulk atoms is as shown in the following table.

No. atoms l in diameter of sphere or edge of cube	$\gamma = \frac{\text{No. surface atoms}}{\text{No. bulk atoms}}$ $\approx 6/l$
10	60%
50	12%
100	6%

Hence taking a middle ground estimate of aggregates as about 50 atoms across, γ is 12% so 12% of all the atoms are in a surface condition. If we take the experimental figure of 1 spin per 250 atoms and ascribe the spins to surface atoms we have 1 spin per 30 surface atoms. This is not unreasonable, and could be analyzed by localized state theory to give the mobility edge[40,44] (energy level outside which pseudostates are localized).

Considerable work has been done where the EPR signal is ascribed to surfaces of voids. The two situations do not differ markedly in principle but the surfaces-of-aggregates hypothesis expects effects on EPR signals from clean films which are subsequently exposed to gases. Such expectations are less marked for voids unless most of them have fissures through to surfaces. More experiments are desirable on this point.

IX. OTHER SEMICONDUCTORS

EPR results are available for vacuum crushed Ge and Gi-Si alloys, reviewed recently,[1] and for amorphous Ge and SiC.[57] In the case of Ge, the number of spins from the powder was, for equal crushed surface areas, about a factor of 10 lower than for Si, and for the films, a factor of 2 lower. Owing to difficulties of proving that particularly treated samples of Ge and Si are properly comparable, these figures are only indications that the spin density for Ge appears to be less than for Si. As with Si, the EPR signal from Ge seems to be very similar for both amorphous films and crushed powders, both in g value (2.021) and width (4 mT). Although no indentation experiments have been performed on Ge (the weaker EPR signals make such experiments very difficult) it seems reasonable, in view of the above similarities, to ascribe the Ge signal to microcracks as well. The effects of oxygen on the Ge signal differ from those on Si, but these are ascribed to differences in chemical interaction in the two cases between the gas and the atoms at the microcracks.

In the case of Ge-Si alloys it is reasonable to assume that the EPR signals from crushed powders (the only types of sample investigated) are also probably due to centers on microcracks. Other materials such as SiC have not been studied sufficiently to make an assessment.

X. CONCLUSION

Mechanical abuse of silicon causes microcracks which give an EPR signal proportional to the crack area. A wide variety of data, including gas exposure effects become explicable for the first time. The resonance centers are thought to be localized states on the surface of the microcracks, localization being induced by spatially varying overlap and stress effects. Clean-cleaved Si surfaces give no EPR signal, due to the pairing of electrons on alternate atomic sites. The resonance from amorphous films might be explicable as due to localized states on surfaces of small aggregates that make up the films.

ACKNOWLEDGMENTS

The authors have had helpful discussions with B. R. Lawn, who kindly loaned indentation equipment, on properties of fractures, and with D. J. Miller on localized state theory. Technical assistance was provided by P. Holmes. This work was supported by the Australian Research Grants Committee and by the U. S. Army Research and Development Group (Far East) under Grant No. DA-CRD-AFE-S92-544-71-6168.

APPENDIX

A number of quantitative and qualitative calculations about the model in Fig. 17 have appeared recently.[2,24-27,29-32] The parameters for the raised surface atoms (0.018 nm elevation) and the lowered atoms (0.011 nm depression) were computed on bulk-consistent energy minimization considerations.[22] It has been stated erroneously,[26,27] based

on incomplete calculations, that these parameters would cause insufficient splitting of the surface-state band in the energy gap. However, a full self-consistent calculation[2] using these parameters gives substantial splitting as shown in Fig. 18, and predicts a surface-state optical absorption peak close to that measured.[28] Hence any modification to the parameters is likely to be minor rather than the large amounts suggested on qualitative grounds.[29] However, the constant bond length that was assumed in order to simplify the computations[22] may need minor charges as suggested recently.[30-32] It should be noted that in the results of Fig. 18, optical transitions from the lower to the upper surface-state band are of reduced probability due to the small spatial overlap of the wave functions corresponding to these bands. However, transitions to the upper band may occur from the bulk valence band as well, so that the total probability could then easily match the experimental data. This would also increase the theoretical energy for the surface optical absorption peak to about 0.45 eV, the measured value.

[1]D. Haneman, Jpn. J. Appl. Phys. Suppl. 2, Pt. 2, 371 (1974).
[2]M. Schlüter, J. Chelikowsky, S. G. Louie, and M. L. Cohen, Phys. Rev. B 12, 4200 (1975).
[3]D. Haneman, Phys. Rev. 170, 705 (1968).
[4]D. Kaplan, D. Lepine, Y. Petroff, and P. Thirry, Phys. Rev. Lett. 35, 1376 (1975).
[5]B. P. Lemke and D. Haneman, Phys. Rev. Lett. 35, 1379 (1975).
[6]M. F. Chung and D. Haneman, J. Appl. Phys. 37, 1879 (1966).
[7]M. F. Chung, J. Phys. Chem. Solids 32, 475 (1971).
[8]S. G. Davison and J. D. Levine, Solid State Physics 25, 1 (1970); H. Ibach and J. E. Rowe, Surface Sci. 43, 481 (1974), and references therein.
[9]W. Mönch, Festkörperprobleme 13, 24 (1973), and references therein; L. F. Wagner and W. E. Spicer, Phys. Rev. B 9, 1512 (1974), and references therein.
[10]D. Haneman, *Characterization of Solid Surfaces*, edited by P. F. Kane and G. B. Larrabee (Plenum, New York, 1974), Chap. 14, p. 337.
[11]D. J. Miller, D. L. Heron, and D. Haneman, J. Vac. Sci. Technol. 9, 906 (1972).
[12]J. T. P. Grant and D. Haneman, Surface Sci. 15, 117 (1969).
[13]R. U. Khokhar and D. Haneman, J. Appl. Phys. 44, 1231 (1973).
[14]B. R. Lawn and M. V. Swain, J. Mat. Sci. 10, 113 (1975).
[15]B. R. Lawn and E. R. Fuller, J. Mat. Sci. 10, 2016 (1975).
[16]G. Feher, Phys. Rev. 114, 1219 (1959).
[17]G. K. Walters and T. L. Estle, J. Appl. Phys. 32, 1854 (1961).
[18]D. Haneman, M. F. Chung, and A. Taloni, Phys. Rev. 170, 719 (1968).
[19]A. Taloni and W. J. Rogers, Surface Sci. 19, 371 (1970).
[20]E. N. Pugh and L. E. Samuels, J. Electrochem. Soc. 111, 1429 (1964).
[21]M. V. Swain, B. R. Lawn, and S. J. Burns, J. Mat. Sci. 9, 175 (1974).
[22]A. Taloni and D. Haneman, Surface Sci. 10, 215 (1968).
[23]For review of experimental data to 1974 see D. Haneman, in *Surface Physics of Phosphors and Semiconductors*, edited by C. G. Scott and C. E. Reed (Academic, New York, 1975), Chap. 1.
[24]H. Ibach and J. E. Rowe, Surface Sci. 43, 481 (1974).
[25]J. E. Rowe and J. C. Phillips, Phys. Rev. Lett. 32, 1315 (1974).
[26]A. Selloni and E. Tosatti, Solid State Commun. 17, 387 (1975).
[27]I. P. Batra and S. Ciraci, Phys. Rev. Lett. 34, 1337 (1975); 36, 170 (1976).
[28]G. Chiarotti, S. Nannarone, R. Pastore, and P. Chiaradia, Phys. Rev. B 4, 3398 (1971); Surface Sci. 54, 547 (1976).
[29]W. A. Harrison, Surface Sci. 55, 1 (1976).
[30]J. A. Appelbaum and D. R. Hamann, Phys. Rev. B 12, 1410 (1975).
[31]F. Yndurian and L. M. Falicov, Solid State Commun. 17, 855 (1975).
[32]K. C. Pandey and J. C. Phillips, Phys. Rev. Lett. 34, 1451 (1975).
[33]J. A. Appelbaum and D. R. Hamann, Phys. Rev. Lett. 31, 106 (1973); 32, 225 (1974); Phys. Rev. B 8, 1777 (1973).
[34]D. Haneman and D. L. Heron, in *The Structure and Chemistry of Solid Surfaces*, edited by G. A. Somorjai (Wiley, New York, 1969), Chap. 24.
[35]D. Haneman, J. T. P. Grant, and R. U. Khokhar, Surface Sci. 13, 119 (1969).
[36]J. W. T. Ridgway and D. Haneman, Surface Sci. 18, 441 (1969).
[37]D. Haneman and E. N. Pugh, J. Appl. Phys. 34, 2269 (1963).
[38]M. Henzler, Surface Sci. 36, 109 (1973).
[39]P. W. Anderson, Phys. Rev. 109, 1492 (1958).
[40]N. F. Mott, Philos. Mag. 22, 7 (1970); 19, 835 (1969).
[41]M. H. Cohen, J. Noncryst. Solids 4, 391 (1970).
[42]J. Ziman, J. Phys. C 2, 1230 (1969).
[43]M. A. Ball, J. Phys. C 4, 1747 (1971).
[44]M. H. Cohen, H. Fritzsche, and S. R. Ovshinsky, Phys. Rev. Lett. 22, 1065 (1969).
[45]R. T. Sanderson, *Chemical Bonds and Bond Energy* (Academic, New York, 1971).
[46]T. A. Kaplan, S. D. Mahanti, and W. M. Hartmann, Phys. Rev. Lett. 27, 1796 (1971).
[47]G. Beni and P. Pincus, Phys. Rev. B 9, 2963 (1974).
[48]R. A. Bari, Phys. Rev. B 3, 2662 (1971).
[49]D. J. Miller (unpublished).
[50]I. Shiota, N. Miyamoto, and Nishizawa, Surface Sci. 36, 414 (1973).
[51]G. Boskovitz and D. Haneman, Surface Sci. 44, 253 (1974).
[52]B. L. Crowder, R. S. Title, M. H. Brodsky, and G. D.

Pettit, Appl. Phys. Lett. 16, 205 (1970).
[53]N. N. Gerasimenko, A. V. Dvurenchenskii, and L. S. Smirnov, Sov. Phys. Semicond. 5, 1487 (1972); 6, 965 (1972).
[54]S. Hasegawa, K. Ichida, and T. Shimizu, Jpn. J. Appl. Phys. 12, 1181 (1973).
[55]G. A. N. Connell and J. R. Pawlik, Phys. Rev. B 13, 787 (1976).
[56]M. H. Brodsky, R. S. Title, K. Weiser, and G. D. Pettit, Phys. Rev. B 1, 1632 (1970).
[57]M. H. Brodsky and R. S. Title, Phys. Rev. Lett. 23, 581 (1969).
[58]Z. Z. Ditina, L. P. Strakhov, and H. H. Helms, Sov. Phys. Semicond. 2, 1006 (1969).
[59]A review is D. Adler, CRC Crit. Rev. Solid State Sci. 318 (1973).
[60]P. G. Le Comber, R. D. Lovelard, W. E. Spear, and R. A. Vaughan, *Amorphous and Liquid Semiconductors* edited by J. Stuke and W. Brenig (Taylor and Francis, London, 1974).

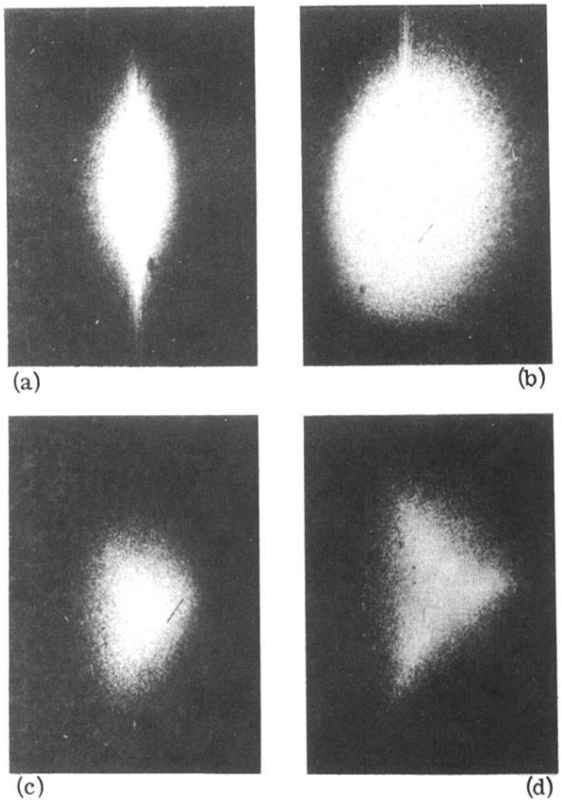

FIG. 11. Appearance on screen of laser beam reflected at normal incidence from mechanically polished Si specimens. Polishing particle sizes in microns, (a) 1, (b) 6, (c) 14, (d) 25.

FIG. 14. Scanning electron micrograph of surfaces of crushed powder particle, showing cracks between regions of different morphology. Width of picture, 240 μm.

(a)

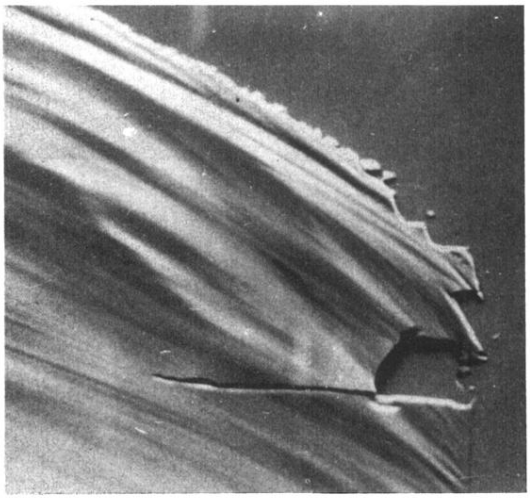

(b)

FIG. 15. (a) Schematic drawing of crack under step. (b) Scanning electron micrograph of steps on cleaved Si surfaces, revealing undercracks where piece chipped off. Width of picture, 200 μm.

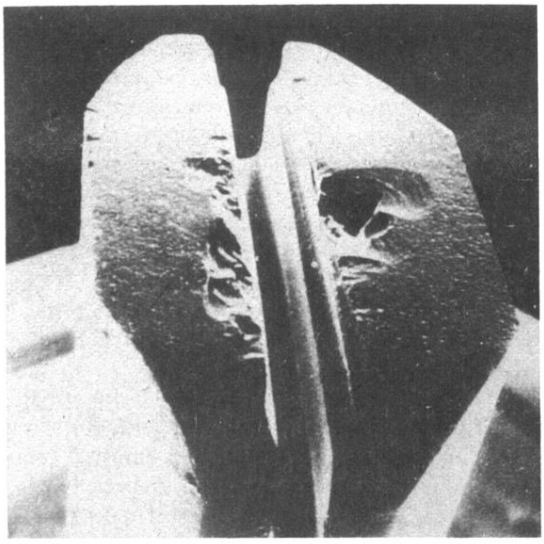

FIG. 16. Scanning electron micrograph of top portion of Si crystal showing chipped region induced by wedge forced into groove. Specimen did not break at groove, but gave EPR signal after this damage. Specimen approximately 5×2 mm^2 cross sectional area.

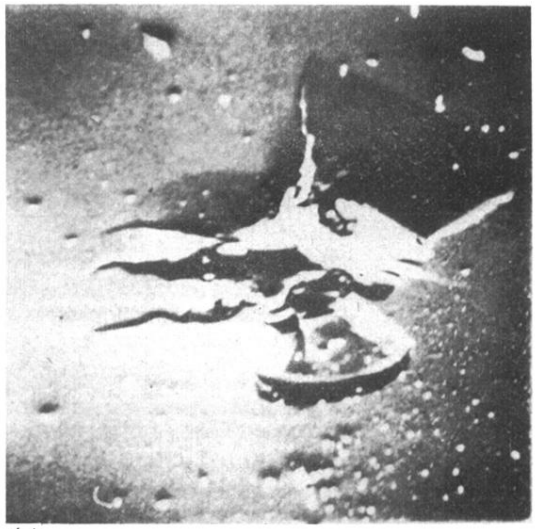

(a)

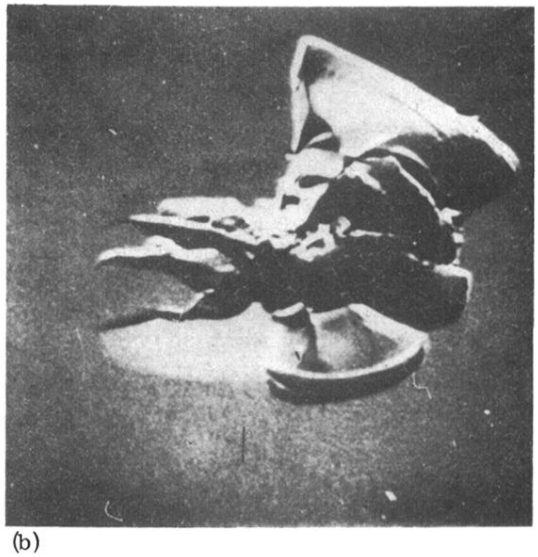

(b)

FIG. 7. Scanning-electron-microscope pictures of diamond point indentation (1 kg load) on (111) Si surface (a) before and (b) after ultrasonic cleaning. Note removal of powder debris and lifting out of portions on lateral vent cracks. Width of micrograph, 0.17 mm.